



Published in final edited form as:

Arch Oral Biol. 2023 January ; 145: 105582. doi:10.1016/j.archoralbio.2022.105582.

Effect of Nystatin on *Candida albicans* - *Streptococcus mutans* Duo-species Biofilms

Nora Alomeir¹, Yan Zeng¹, Ahmed Fadaak¹, Tong Tong Wu², Hans Malmstrom¹, Jin Xiao¹

¹Eastman Institute for Oral Health, University of Rochester Medical Center, Rochester, USA

²Department of Biostatistics and computational biology, University of Rochester Medical Center, Rochester, USA

Abstract

Objective: To assess the effect of Nystatin on *Candida albicans* and *Streptococcus mutans* duo-species biofilms using an *in vitro* cariogenic biofilm model.

Design: Biofilms were formed on saliva-coated hydroxyapatite discs under high sugar challenge (1% sucrose and 1% glucose), with inoculation of 10⁵CFU/ml *S. mutans* and 10³CFU/ml *C. albicans*. Between 20–68 hours, biofilms were treated with 28,000 IU Nystatin solution, 5 minutes/application, 4 times/day, to mimic the clinical application. Biofilm's three-dimensional structure was assessed using multi-photon confocal microscopy. The expression of *C. albicans* and *S. mutans* virulence genes was assessed via real-time PCR. Duplicate discs were used in 3 independent repeats. *t*-test and Mann-Whitney U test were used to compare outcomes between treatment and control group.

Results: Nystatin treatment eliminated *C. albicans* in biofilms at 44 hours. Nystatin-treated group had a significant reduction of biofilm dry-weight and reduced *S. mutans* abundance by 0.5 log CFU/ml at 44 and 68 hours (p<0.05). Worth noting that biomass distribution across the vertical layout was altered by Nystatin treatment, resulting in less volume on the substrate layers in Nystatin-treated biofilms compared to the control. Reduction of microcolonies size and volume was also observed in Nystatin-treated biofilms (p<0.05). Nystatin-treated biofilms formed

Corresponding Author: Jin Xiao DDS, MS, PhD, Associate Professor, Director, Perinatal Oral Health, Eastman Institute for Oral Health, University of Rochester, 625 Elmwood Ave, Rochester, USA, 14620, jin_xiao@urmc.rochester.edu, Phone: +1 585-273-1957. Author contributions

Nora Alomeir contributed to the study design, data acquisition and analysis, data interpretation, manuscript writing and critical revision of the manuscript. Yan Zeng contributed to data acquisition and analysis, data interpretation, manuscript writing and critical revision of the manuscript. Ahmed Fadaak contributed to data acquisition, data interpretation, and critical revision of the manuscript. Tong Tong Wu contributed to the study design, data analysis, data interpretation, manuscript writing and critical revision of the manuscript. Hans Malmstrom contributed to the study design, data interpretation, and critical revision of the manuscript. Jin Xiao contributed to the study design, data acquisition and analysis, data interpretation, manuscript writing and critical revision of the manuscript.

Publisher's Disclaimer: This is a PDF file of an unedited manuscript that has been accepted for publication. As a service to our customers we are providing this early version of the manuscript. The manuscript will undergo copyediting, typesetting, and review of the resulting proof before it is published in its final form. Please note that during the production process errors may be discovered which could affect the content, and all legal disclaimers that apply to the journal pertain.

Statement of Ethics

An ethics statement was not required for this study type, no human or animal subjects or materials were used.

Conflict of Interest Statement

The authors declared no potential conflicts of interest.

unique halo-shaped microcolonies with reduced core EPS coverage. Furthermore, Nystatin-treated biofilms had significant down-regulations of *S. mutans gtfD* and *atpD* genes ($p < 0.05$).

Conclusions: Nystatin application altered the formation and characteristics of *C. albicans* and *S. mutans* duo-species biofilms. Therefore, developing clinical regimens for preventing or treating dental caries from an antifungal perspective is warranted.

Keywords

Fungi; Bacteria; Antifungal; *Streptococcus mutans*; Biofilm

Introduction

Candida albicans is the most common fungal human pathogen causing localized and systemic infections in humans (Talapko et al., 2021). Young children often have a history of fungal infection in their early life; for example, the medical records of 196 1–3 years old American children indicated past histories of diaper rash (7%), oral candidiasis (6%), anemia (2%), and facial rash (2%) (Jabra-Rizk et al., 2007). The oral carriage of *candida* organisms is reported to be 45–65% in healthy children and 45% in neonates (Patil et al., 2015). During a routine oral exam, a study revealed that 66% of those 196 children had fungal growth in the samples collected from the mid-dorsum of the tongue, with most of the isolates being *C. albicans* (Jabra-Rizk et al., 2007).

Intriguingly, previous studies reported that the prevalence of *C. albicans* in children with early childhood caries (ECC) was higher than in caries-free children (Xiao et al., 2018). The carriage of *C. albicans* was also positively associated with the carriage of *Streptococcus mutans* in the saliva and plaque samples of children with ECC (Xiao et al., 2018). A review by Koo and his colleagues highlighted a synergistic interaction between *C. albicans* and *S. mutans* mediated by *S. mutans*-derived glucosyltransferases (GTFs) (Koo et al., 2018). With the presence of sucrose, the GtfB enzyme binds to the cell surface of *C. albicans* and involves synthesizing exopolysaccharides (EPS), mainly insoluble α -glucan (Hwang et al., 2017). EPS mediates the binding interaction between *C. albicans* and *S. mutans* and further promotes interspecies biofilm formation (Koo et al., 2018). Furthermore, the presence of *C. albicans* and *S. mutans* leads to more severe dental caries in an animal model (Falsetta et al., 2014) and is associated with a higher prevalence of caries in children (Eidt et al., 2020). Due to the cross-kingdom interaction in the context of dental caries, an antifungal regimen might be able to control *S. mutans*, thus preventing ECC via controlling oral yeast infections.

The antifungal medications for treating oral candidiasis include two main groups -polyenes and azole (Scheibler et al., 2018). Fluconazole, one of the Azoles, is a broadly used antifungal agent to treat systemic fungal infections (Govindarajan et al., 2022). A recent study assessed the effect of Fluconazole and povidone-iodine on the disruption of *C. albicans*-*S. mutans* duo-species biofilms; this study provided compelling evidence that targeting bacterial EPS is a critical factor for enhanced antifungal drug efficacy in mixed kingdom biofilms (Kim et al., 2018). Among the polyene group, Nystatin is the most commonly used medication to treat oral candidiasis (Garcia-Cuesta et al., 2014). Moreover,

Nystatin is an antimicrobial agent with both fungicidal and fungistatic properties (Scheibler et al., 2018).

The topical use of Nystatin is considered the most common route of administration in dentistry, as systemic exposure is minimal (Lyu et al., 2016; Pappas et al., 2016). The commonly recommended dose for Nystatin topical use is 200,000–600,000 IU (four times a day, qid) for children and adults, and 100,000–200,000 IU qid for newborns and infants (Lyu et al., 2016). Treatment duration varies from 1 or 2 to 4 weeks (Lyu et al., 2016). Nystatin is well tolerated because of its poor absorption in the gastrointestinal tract (Garcia-Cuesta et al., 2014). In addition, Nystatin has minimal side effects (such as Nausea and vomiting) and a low risk of hepatotoxicity, compared to Fluconazole, in which hepatotoxicity was reported in rare cases due to its systemic exposure (Garcia-Cuesta et al., 2014).

To our knowledge, no studies have assessed the effect of Nystatin on the interaction of *S. mutans* and *C. albicans* *in vitro* and *in vivo*. Therefore, our immediate goal was to assess the effectiveness of using Nystatin to inhibit the formation of *C. albicans*-*S. mutans* duo-species biofilms using an established *in vitro* model, which would provide rationale for conducting further studies using multi-species biofilm *in vitro* model, *in situ* model and in clinical trials.

Materials and Methods

The overall Study design is demonstrated in Fig. 1; detailed study methods are described below. All assays were repeated in three independent experiments.

Bacterial strains and growth conditions

In this study, *S. mutans* UA159 (ATCC 700610), a proven virulent cariogenic dental pathogen (Ajdic et al., 2002), and *C. albicans* SC5314 were used to form duo-species biofilms. We selected *C. albicans* in addition to *S. mutans* because this fungus is frequently detected in the supragingival plaque of children with dental caries (Xiao et al., 2018).

Using a batch culture approach, saliva-coated hydroxyapatite (sHA) discs were utilized to mimic the formation of biofilms according to the “ecological plaque-biofilm” concept (Marsh, 2003), as described by Xiao *et al.* (Xiao et al., 2012). The bacterial strains were recovered from frozen stock on blood agar (TSA with Sheep Blood, Thermo Scientific™ R01202) and were incubated for 48 hours (5% CO₂, 37°C). Then, 3–5 colonies of each species were inoculated into 10 ml of broth for overnight incubation (5% CO₂, 37°C). *C. albicans* cells were grown in YPD broth (BD Difco™, 242820), and *S. mutans* cells were grown in TSBYE broth (3% Tryptic Soy, 0.5% Yeast Extract Broth, BD Bacto™ 286220 and Gibco™ 212750) with 1% glucose at 37°C and 5% CO₂.

On the following day, 0.5 ml of the overnight starters were added to an individual glass tube containing fresh broth and incubated for 3–4 hours to the mid-exponential phase until an optimal optical density OD₆₀₀ of 0.80 for *C. albicans* and 1.00 for *S. mutans* was reached. These two bacterial suspensions were then mixed to produce an inoculum containing *S. mutans* (10⁵ CFU/ml) and *C. albicans* (10³ CFU/ml) to mimic the clinical carriage of *S.*

mutans and *C. albicans* in children with early childhood caries. It is also critical for the reproducibility of our model (Koo et al., 2010).

Duo-species biofilm model

Duo-species biofilms were formed on saliva-coated hydroxyapatite discs (1.25 cm diameter, Clarkson Chromatography Products, Inc., South Williamsport, PA) (Koo et al., 2005; Koo et al., 2010), which were vertically positioned using custom-made disc holders, in order to imitate the position of natural teeth. The mixed population of *S. mutans* and *C. albicans* were inoculated in 2.8 ml of TSBYE with 0.1% (w/v) sucrose and incubated at 37°C and 5% CO₂. During the first 20 h, the organisms were grown undisturbed to allow initial biofilm formation and mimic the clinical condition that *C. albicans* and *S. mutans* already present in the oral cavity. At 20 h of biofilm growth, the biofilms were transferred to TSBYE that contains 1% (w/v) sucrose or 1% (w/v) glucose to introduce a cariogenic challenge, while an additional set of biofilms were grown in TSBYE with 0.1% (w/v) sucrose. The culture medium was replaced once daily (every 24 h) until the end of the experimental period (68 h). Duplicate discs were used in 3 independent repeats for accuracy and reproducibility, a total of 6 discs were used for each biofilm condition (n=6).

The culture medium pH was measured daily using a standard pH electrode. The biofilms were analyzed at specific time points using confocal imaging/fluorescence and biochemical assays (Fig. 1).

Nystatin Treatment

2.8 ml of 10,000 unit/mL Nystatin suspension in DPBS (Sigma-Aldrich, BioReagent, Saint Louis, MO, USA) was used for each treatment. The biofilms formed on the sHA discs were treated in Nystatin suspension for 5 minutes, four times/day (detailed treatment regimen see Fig. 1). After each treatment, HA discs were dip-washed in sterile Dulbecco's phosphate-buffered saline (DPBS) to remove excess agents, and then transferred back to the culture medium. DPBS solution was also used as a topical treatment for the control group.

Viable cells in biofilms

The biofilms were removed from the discs and resuspended in sterile 0.89% (w/v) NaCl solution. The solution was homogenized by sonication (30-sec pulse at an output of 7W; Branson Sonifier 150, Branson Ultrasonics, Danbury, CT) without killing bacterial species from sonication (Koo et al., 2010). The homogenized suspension was plated on blood agar using an automated EddyJet Spiral Plater (IUL, SA, Barcelona, Spain) to determine the colony-forming units (CFU), which reflect the number of viable cells. The two species were differentiated by observation of colony morphology in conjunction with microscopic examination of cells from selected colonies (Guggenheim et al., 2001). The homogenized biofilm suspension was also used for the measurement of dry weight detailed previously (Zeng et al., 2019).

Laser scanning confocal fluorescence microscopy (LCSFM) imaging of biofilm matrix

We examined the three-dimensional (3D) structure of intact biofilms by directly incorporating fluorescent markers during the synthesis of the extracellular polysaccharide

(EPS) matrix using LCSFM (Klein et al., 2009; Klein et al., 2011). Hence, 1 μ M Alexa Fluor[®] 647-labeled dextran conjugate (molecular weight, 10 kDa; absorbance/fluorescence emission maxima of 647/668 nm; Molecular Probes, Invitrogen Corp., Carlsbad, CA) was added to the culture medium starting from the biofilm formation to the biofilm development for EPS visualization. This fluorescent marker does not stain the bacterial cells used in our study using a specific concentration (Klein et al., 2009). Both bacterial and fungal species in the biofilms were labeled by SYTO[®] 9 green, fluorescent nucleic acid stain (485/498 nm; Molecular Probes) following a standard protocol (Klein et al., 2009; Klein et al., 2011). The images were taken using Olympus FV 1000 two-photon laser scanning microscope (Olympus, Tokyo, Japan) that contains a 10X (0.45 numerical aperture) or 25X LPlan N (1.05 numerical aperture) water immersion objective lens (Koo et al., 2010). Each HA disc with biofilm was scanned at five random positions selected at the microscope stage (Xiao & Koo, 2010), and confocal image series were generated. A total of 10 image stacks were obtained for each biofilm condition.

Computational analyses of the confocal biofilm images

We analyzed the confocal images with a specific software that simultaneously visualizes and quantifies EPS and bacterial cells within intact biofilms (Klein et al., 2011). Therefore, Amira 5.0.2 (Mercury Computer Systems Inc., Chelmsford, MS) was used to visualize the morphology and 3D architecture of both structural components of biofilms (EPS and bacteria) as detailed previously (Klein et al., 2011; Xiao & Koo, 2010). The quantitative analysis of the images was carried out using COMSTAT and DUOSTAT scripts (<http://www.imageanalysis.dk>). We used COMSTAT to calculate the biomass of bacteria and EPS components, the number, thickness, and layer distribution of biofilms. In addition, COMSTAT quantifies the size (volume, diameter, and height) of surface-attached and floating microcolonies, as detailed elsewhere (Heydorn et al., 2000; Xiao & Koo, 2010). We used DUOSTAT to calculate the co-localization of EPS and bacterial cells within the 3D biofilm structure (Klein et al., 2011).

Real-time PCR

Real-time PCR was performed to assess the expression of *C. albicans* and *S. mutans* virulence genes. We collected biofilms from four discs at six points, 20, 24, 30, 44, 48, and 54 h, for both the control group and the Nystatin-treated group (Fig. 5–6). The discs were immersed in RNAlater (AppliedBiosystems/Ambion, Austin, TX, USA) for 1 hour, followed by biofilms removal with a spatula. RNA extraction and purification were completed using MasterPure complete DNA and RNA purification kit (Epicentre, Lucigen, WI, USA). The raw RNA product was then quantified using NanoDrop One Microvolume UV-Vis Spectrophotometer (Thermo Scientific[™], Wilmington, DE, USA). Depletion of rRNA was performed using Ribozero rRNA Removal Kit (Illumina, San Diego, CA, USA).

The cDNA synthesis was completed from 0.2 mg of purified RNA with the Bio-Rad iScript cDNA synthesis kit (Bio-Rad Laboratories, Inc., Hercules, CA). Amplification of *S. mutans* and *C. albicans* genes was conducted using Applied Biosystems[™] PowerTrack[™] SYBR Green Master Mix and a QuantStudio[™] 3 Real-Time PCR System (Thermo FisherScientific, USA). For *S. mutans* and *C. albicans* genes comparative calculation, we used reference

genes: *gyrA* for *S. mutans* (Zeng & Burne, 2013) and ACT1 for *C. albicans*. For *C. albicans* virulence genes, the hyphae-specific genes (HWP1, and ECE1), manganese-dependent superoxide dismutase (SOD3) (Martchenko et al., 2004), chitinase gene (CHT2) (McCreath et al., 1995), and ergosterol Biosynthesis gene (ERG4) were analyzed. For *S. mutans* virulence genes, the target genes were Gtf genes (*gtfB*, *gtfC*, and *gtfD*) responsible for cellular adhesion (Ooshima et al., 2001), enolase gene (*eno*), and ATPase gene (*atpD*). Methods were detailed previously (Zeng et al., 2022). The genes and primers used are listed in Table S1.

Statistical analysis

The CFU value for *S. mutans* and *C. albicans* were converted to a natural log for statistical analysis. The normality of numerical values (CFU natural log value, biomass of bacteria and EPS, number and size of microcolonies, pH value of the culture medium, and gene expression ratio) was assessed. *t*-test was performed to compare the difference between the control and Nystatin treatment group for normally distributed data, and Mann-Whitney U test was used to assess the differences for non-normal data. Repeated ANOVA was used to assess the *S. mutans* virulence genes expression between different time points among the control and Nystatin-treated group. Statistical analyses were performed using IBM SPSS.

Results

The effect of Nystatin on duo-species biofilm was assessed using a duo-species biofilm model (Fig. 1). Nystatin treatment eliminated *C. albicans* after 44 hours of biofilm formation compared to the control group (Fig. 2A). Intriguingly, the Nystatin-treated biofilms formed in a higher sugar condition (1% sucrose) had a significant reduction of dry weight ($p < 0.05$) (Fig. 3B). The 1% sucrose sugar condition reflected a high cariogenic challenge. In addition, the abundance of *S. mutans* was reduced by 0.5 log CFU/ml at 44 and 68 hours in the Nystatin-treated group with 1% sucrose ($p < 0.05$).

Inhibitory effect of Nystatin on biofilm formation

We observed the biofilm closely using a two-photon laser confocal microscope to explore the Nystatin treatment's effect further. COMSTAT and DUOSTAT were used to determine the biofilm's three-dimensional structure parameters (biomass of bacteria and EPS, thickness/layer distribution of biofilms, and formation of surface-attached and floating microcolonies). The biomass and average thickness of bacteria and EPS was lower in the treatment group than in the control group (Fig. 3A). Biofilms formed in the control group had a dense EPS layer covering the sHA disc. Worth noting that the biomass distribution across the vertical biofilm layout was altered by Nystatin treatment, resulting in less volume on the substrate layers of the Nystatin group compared to the control group (Fig. 3C and D).

The biofilms treated with Nystatin formed unique halo-shaped microcolonies with reduced core EPS coverage (red) (Fig. 3A). We also observed smaller microcolonies (green) in the Nystatin-treated group, which can be seen clearly in the cross-sectional view. Reduction of the number and size of floating and attached microcolonies in the Nystatin treatment group was also confirmed from the quantitative assessment via COMSTAT (Table 1). The amount

of bacteria co-localization by EPS was quantified using DUOSTAT, which confirms the findings of the representative confocal images.

Changes in culture media pH

The culture media pH was measured at three different time points during the biofilm experiment. The acidity of the spent culture medium was significantly lower in the Nystatin-treated group compared to the control group at 44 and 68 hours under 0.1% sucrose sugar conditions (Fig. 4A). However, the acidity of the control and treatment group was similar at 44 and 68 hours under 1% sucrose and 1% glucose sugar conditions (Fig. 4B–C).

Expression of virulence genes

We performed real-time PCR to assess *C. albicans* and *S. mutans* virulence genes. For *C. albicans*, virulence genes (*CHT2*, *HWPI*, *ECE1*, and *ERG4*) were significantly down-regulated ($p < 0.05$) immediately following the first Nystatin application at 24h; *SOD3* gene was significantly down-regulated ($p < 0.05$) after 30 hours (see Fig. 5). At 44 hours which is after 4 applications of Nystatin, expression was not detected for all *C. albicans* virulence genes, which is consistent with our results in (Fig. 2) where no viable *C. albicans* cells were cultured at 44h biofilms in the Nystatin treatment group.

The biofilms treated with Nystatin had down-regulations of *S. mutans gtfB*, and *eno* genes compared to the control group, despite no statistically significant differences being between the control and treatment group (Fig. 6). However, at 44 hours, and 4 Nystatin applications, *gtfD* and *atpD* were down-regulated and statistical difference ($p < 0.05$) was noted.

We further assessed the dynamic expression of *S. mutans* virulence genes in control and Nystatin-treated biofilms. No significant change was seen in the dynamic expression of *gtfB*, *atpD*, and *eno* genes in both the control and Nystatin-treatment group. However, there was a significant change ($p < 0.05$) in the dynamic expression of *gtfD* in the control group (Fig. 7A) and a significant change in the dynamic expression of *gtfC* in the Nystatin-treated biofilms (Fig. 7B).

Discussion

Given that limited studies have assessed the effect of an antifungal regimen on inhibiting *C. albicans* and *S. mutans* biofilms, our study sheds new light on *C. albicans*-*S. mutans* duo-species biofilm control from a fungal perspective. In our biofilm model, Nystatin eliminated *C. albicans* after 44 hours of biofilm formation, with a significant down-regulation of several virulence genes immediately following Nystatin application. For instance, the hyphae-specific genes (*HWPI* and *ECE1*) were significantly down-regulated at 30 h and the expression of *HWPI* and *ECE1* was not detectable after 44 h. The expression of other *C. albicans* genes, such as manganese-dependent superoxide dismutase (*SOD3*) (Martchenko et al., 2004), chitinase gene (*CHT2*) (McCreath et al., 1995), and ergosterol Biosynthesis gene (*ERG4*) was also undetected after 4 applications of Nystatin at 44 h.

The reduction of *C. albicans* in the biofilms was associated with a 0.5 log reduction in *S. mutans* viable count (CFU/ml). Less *S. mutans* viable cells in the Nystatin-treated biofilms

could be partially explained by the down-regulation of *eno* (acid production) and *atpD* (acid tolerance) (Jung et al., 2022). Furthermore, a significant reduction in biofilm dry weight was seen in the Nystatin-treated group compared to the control group under the most cariogenic sugar condition (1% sucrose). Nystatin-treated biofilms had reduced biomass and modified biofilm architecture that is less virulent, with fewer and smaller substrate attached microcolonies. The *gtfB* is associated with insoluble glucan synthesis and the formation of the backbone of cariogenic biofilms (Koo et al., 2010). Despite a statistically non-significant difference in *gtfB/C* expression in the Nystatin-treated biofilms compared to the control group, a trend of down-regulation of *gtfB* expression after the Nystatin application was seen. The *GtfD* enzyme produces soluble glucans and collaborates with the other Gtf enzymes (*GtfB* and *GtfC*) to promote adherence of bacterial cells and biofilm formation in the oral cavity (Matsumoto-Nakano, 2018). We also see a statistically significant reduction of *gtfD* expression at 44h (after 4 applications of Nystatin). Despite the positive reduction of *S. mutans* in relation to the *C. albicans* reduction, it is worth noting 0.5 log reduction of *S. mutans* is below the desirable 3 log₁₀ reduction for considering a product for being clinically relevant, according to the American Society of Microbiology (Petersen et al., 2007).

Moreover, Nystatin-treated biofilm formed unique halo-shaped microcolonies with reduced EPS in the core of the microcolonies. Since the microcolony structure in biofilms is often associated with oral biofilm virulence, such as acting as barriers to environmental challenges (shear force, application of antimicrobial agents) and forming an acidic environment that leads to more severe demineralization of enamel surfaces (Xiao et al., 2017; Xiao et al., 2012), further understanding of the Nystatin-treatment related halo-shaped microcolonies should be conducted in the future.

A recent study (Kim et al., 2018) examined the effect of using an antifungal regimen (Fluconazole) on duo-species biofilm *in vitro* and *in vivo*, reporting a significant reduction in *S. mutans* and *C. albicans* viable count compared to the control group, however, Fluconazole did not eliminate the viable cells of *C. albicans*. Our study observed a complete elimination of *C. albicans* viable cells, which might be due to the washing action of Nystatin suspension compared to the systemically taken antifungal medication fluconazole. In addition, the significant reduction in *S. mutans* after the topical application with fluconazole correlates with our findings as Nystatin reduced the abundance of *S. mutans* as well. In addition, *C. albicans* serve as a surface for *S. mutans* to bind and form biofilms. Hwang and his colleagues report that mannans located on the outer surface of *C. albicans* cell wall mediate the binding of *S. mutans*-derived enzyme GtfB, enhance glucan-matrix production and modulate bacterial-fungal association within biofilms (Hwang et al., 2017; Hwang et al., 2015). Reduction of *C. albicans* in the biofilm system could reduce *S. mutans* binding due to the abovementioned *S. mutans-C. albicans* binding interactions.

A noteworthy finding is that we observed a significant reduction in culture media pH in the Nystatin-treated group with 0.1% sucrose, compared to the control group, at 44 and 68 hours (Fig. 4A). This finding is in line with a previous study by Willem et al., where growing *C. albicans* in duo-species biofilms (*C. albicans* and *S. mutans*) led to a higher culture medium pH at 24 hours compared to *S. mutans* single-species biofilms (Willems et al., 2016). When

grown alone or in combination, the metabolic productions of *S. mutans* and *C. albicans* deserve further investigation to better understand their synergistic relation.

In addition to Nystatin tested in our study, other antifungal agents to be tested include caspofungin. Caspofungin belongs to the echinocandin family and has a unique mechanism of action by inhibiting the synthesis of $\beta(1-3)$ glucan, a critical component of fungal cell walls (Katzung et al., 2015). In an *in vitro* study investigating the effect of caspofungin on *C. albicans* biofilms, the results suggested that the therapeutic dosage of this agent showed potent activity against *C. albicans* biofilms (Bachmann et al., 2002). Due to its potent effect and unique mechanism of action merits further investigation of caspofungin on other biofilm-associated diseases such as dental caries. Furthermore, recent advanced probiotic research revealed a remarkable inhibitory effect of *Lactobacillus* spp. on *S. mutans* and *C. albicans* duo-species biofilm formation (Zeng et al., 2022). Conjunction of using probiotics and antifungal medication could lead to simultaneous and optimal control of *S. mutans* and *C. albicans*.

Studying multispecies biofilm *in vitro* is critical to understanding oral infectious disease and related management. However, limitations exist from using *in vitro* models. For example, although our biofilm model mimicked a high caries risk condition and supplied a high sugar challenge, our model did not introduce a flow cell setting, which does not mimic clinical shear force, salivation, etc. In addition, this study tested the wild type of *S. mutans* and *C. albicans*, which does not reflect the full spectrum of clinical isolates virulence; further studies are needed to assess the responses of clinical isolates. Furthermore, the current study focused on assessing *C. albicans*; future studies could expand the attention and assessment of the cariogenic role of other *Candida* species, such as *C. dubliniensis*. Future studies are also required to analyze Nystatin's effect in animal models and clinical trials.

Conclusions

Nystatin altered the formation and characteristics of *C. albicans* and *S. mutans* duo-species biofilms. Future studies that investigate the effect of Nystatin on *C. albicans-S. mutans* multi-species biofilms via *in vitro/in situ* models and clinical trials are critical to providing further rationale for developing clinical regimens for preventing or treating dental caries from an antifungal perspective.

Supplementary Material

Refer to Web version on PubMed Central for supplementary material.

Acknowledgement

This study was supported by the NIH National Institute of Dental and Craniofacial Research grant K23DE027412 and R01DE031025. The funding agencies had no role in the study design, data collection, analyses, decision to publish, or preparation of the manuscript.

Data Availability Statement

All data generated or analyzed during this study are included in this article. Further enquiries can be directed to the corresponding author.

References:

- Ajdic D, McShan WM, McLaughlin RE, Savic G, Chang J, Carson MB, Primeaux C, Tian R, Kenton S, Jia H, Lin S, Qian Y, Li S, Zhu H, Najjar F, Lai H, White J, Roe BA, & Ferretti JJ (2002, Oct 29). Genome sequence of *Streptococcus mutans* UA159, a cariogenic dental pathogen. *Proc Natl Acad Sci U S A*, 99(22), 14434–14439. 10.1073/pnas.172501299 [PubMed: 12397186]
- Bachmann SP, VandeWalle K, Ramage G, Patterson TF, Wickes BL, Graybill JR, & Lopez-Ribot JL (2002, Nov). In vitro activity of caspofungin against *Candida albicans* biofilms. *Antimicrob Agents Chemother*, 46(11), 3591–3596. 10.1128/AAC.46.11.3591-3596.2002 [PubMed: 12384370]
- Eidt G, Waltermann EDM, Hilgert JB, & Arthur RA (2020, Nov). *Candida* and dental caries in children, adolescents and adults: A systematic review and meta-analysis. *Arch Oral Biol*, 119, 104876. 10.1016/j.archoralbio.2020.104876 [PubMed: 32905885]
- Falsetta ML, Klein MI, Colonne PM, Scott-Anne K, Gregoire S, Pai CH, Gonzalez-Begne M, Watson G, Krysan DJ, Bowen WH, & Koo H (2014, May). Symbiotic relationship between *Streptococcus mutans* and *Candida albicans* synergizes virulence of plaque biofilms in vivo. *Infect Immun*, 82(5), 1968–1981. 10.1128/IAI.00087-14 [PubMed: 24566629]
- Garcia-Cuesta C, Sarrion-Perez MG, & Bagan JV (2014, Dec). Current treatment of oral candidiasis: A literature review. *J Clin Exp Dent*, 6(5), e576–582. 10.4317/jced.51798 [PubMed: 25674329]
- Govindarajan A, Bistas KG, Ingold CJ, & Aboeed A (2022). Fluconazole. In *StatPearls*. <https://www.ncbi.nlm.nih.gov/pubmed/30725843>
- Guggenheim B, Giertsen E, Schupbach P, & Shapiro S (2001, Jan). Validation of an in vitro biofilm model of supragingival plaque. *J Dent Res*, 80(1), 363–370. http://www.ncbi.nlm.nih.gov/entrez/query.fcgi?cmd=Retrieve&db=PubMed&dopt=Citation&list_uids=11269730 [PubMed: 11269730]
- Heydorn A, Nielsen AT, Hentzer M, Sternberg C, Givskov M, Ersboll BK, & Molin S (2000, Oct). Quantification of biofilm structures by the novel computer program COMSTAT. *Microbiology*, 146 (Pt 10), 2395–2407. 10.1099/00221287-146-10-2395 [PubMed: 11021916]
- Hwang G, Liu Y, Kim D, Li Y, Krysan DJ, & Koo H (2017, Jun). *Candida albicans* mannans mediate *Streptococcus mutans* exoenzyme GtfB binding to modulate cross-kingdom biofilm development in vivo. *PLoS Pathog*, 13(6), e1006407. 10.1371/journal.ppat.1006407 [PubMed: 28617874]
- Hwang G, Marsh G, Gao L, Waugh R, & Koo H (2015, Sep). Binding Force Dynamics of *Streptococcus mutans*-glucosyltransferase B to *Candida albicans*. *J Dent Res*, 94(9), 1310–1317. 10.1177/0022034515592859 [PubMed: 26138722]
- Jabra-Rizk MA, Torres SR, Rambob I, Meiller TF, Grossman LK, & Minah G (2007, Summer). Prevalence of oral *Candida* species in a North American pediatric population. *J Clin Pediatr Dent*, 31(4), 260–263. 10.17796/jcpd.31.4.820968206675v577 [PubMed: 19161062]
- Jung HY, Cai JN, Yoo SC, Kim SH, Jeon JG, & Kim D (2022, Feb 7). Collagen Peptide in a Combinatorial Treatment with *Lactobacillus rhamnosus* Inhibits the Cariogenic Properties of *Streptococcus mutans*: An In Vitro Study. *Int J Mol Sci*, 23(3). 10.3390/ijms23031860
- Katzung BG, Trevor AJ, & Kruidering-Hall M (2015). *Pharmacology: Examination & Board Review* (11th ed.).
- Kim D, Liu Y, Benhamou RI, Sanchez H, Simon-Soro A, Li Y, Hwang G, Fridman M, Andes DR, & Koo H (2018, Jun). Bacterial-derived exopolysaccharides enhance antifungal drug tolerance in a cross-kingdom oral biofilm. *ISME J*, 12(6), 1427–1442. 10.1038/s41396-018-0113-1 [PubMed: 29670217]
- Klein MI, Duarte S, Xiao J, Mitra S, Foster TH, & Koo H (2009, Feb). Structural and molecular basis of the role of starch and sucrose in *Streptococcus mutans* biofilm development. *Appl Environ Microbiol*, 75(3), 837–841. <https://doi.org/AEM.01299-08> [pii] 10.1128/AEM.01299-08 [PubMed: 19028906]

- Klein MI, Xiao J, Heydorn A, & Koo H (2011, Jan 25). An analytical tool-box for comprehensive biochemical, structural and transcriptome evaluation of oral biofilms mediated by mutans streptococci. *J Vis Exp* (47). 10.3791/2512
- Koo H, Andes DR, & Krysan DJ (2018, Dec). *Candida*-streptococcal interactions in biofilm-associated oral diseases. *PLoS Pathog*, 14(12), e1007342. 10.1371/journal.ppat.1007342 [PubMed: 30543717]
- Koo H, Schobel B, Scott-Anne K, Watson G, Bowen WH, Cury JA, Rosalen PL, & Park YK (2005, Nov). Apigenin and tt-farnesol with fluoride effects on *S. mutans* biofilms and dental caries. *J Dent Res*, 84(11), 1016–1020. 10.1177/154405910508401109 [PubMed: 16246933]
- Koo H, Xiao J, Klein MI, & Jeon JG (2010, Jun). Exopolysaccharides produced by *Streptococcus mutans* glucosyltransferases modulate the establishment of microcolonies within multispecies biofilms. *J Bacteriol*, 192(12), 3024–3032. 10.1128/JB.01649-09 [PubMed: 20233920]
- Lyu X, Zhao C, Yan ZM, & Hua H (2016). Efficacy of nystatin for the treatment of oral candidiasis: a systematic review and meta-analysis. *Drug Des Devel Ther*, 10, 1161–1171. 10.2147/DDDT.S100795
- Marsh PD (2003, Feb). Are dental diseases examples of ecological catastrophes? *Microbiology*, 149(Pt 2), 279–294. 10.1099/mic.0.26082-0 [PubMed: 12624191]
- Martchenko M, Alarco AM, Harcus D, & Whiteway M (2004, Feb). Superoxide dismutases in *Candida albicans*: transcriptional regulation and functional characterization of the hyphal-induced SOD5 gene. *Mol Biol Cell*, 15(2), 456–467. 10.1091/mbc.e03-03-0179 [PubMed: 14617819]
- Matsumoto-Nakano M (2018, Feb). Role of *Streptococcus mutans* surface proteins for biofilm formation. *Jpn Dent Sci Rev*, 54(1), 22–29. 10.1016/j.jdsr.2017.08.002 [PubMed: 29628998]
- McCreath KJ, Specht CA, & Robbins PW (1995, Mar 28). Molecular cloning and characterization of chitinase genes from *Candida albicans*. *Proc Natl Acad Sci U S A*, 92(7), 2544–2548. 10.1073/pnas.92.7.2544 [PubMed: 7708682]
- Ooshima T, Matsumura M, Hoshino T, Kawabata S, Sobue S, & Fujiwara T (2001, Jul). Contributions of three glycosyltransferases to sucrose-dependent adherence of *Streptococcus mutans*. *J Dent Res*, 80(7), 1672–1677. 10.1177/00220345010800071401 [PubMed: 11597030]
- Pappas PG, Kauffman CA, Andes DR, Clancy CJ, Marr KA, Ostrosky-Zeichner L, Reboli AC, Schuster MG, Vazquez JA, Walsh TJ, Zaoutis TE, & Sobel JD (2016, Feb 15). Clinical Practice Guideline for the Management of Candidiasis: 2016 Update by the Infectious Diseases Society of America. *Clin Infect Dis*, 62(4), e1–50. 10.1093/cid/civ933 [PubMed: 26679628]
- Patil S, Rao RS, Majumdar B, & Anil S (2015). Clinical Appearance of Oral *Candida* Infection and Therapeutic Strategies. *Front Microbiol*, 6, 1391. 10.3389/fmicb.2015.01391 [PubMed: 26733948]
- Petersen PJ, Jones CH, & Bradford PA (2007, Nov). In vitro antibacterial activities of tigecycline and comparative agents by time-kill kinetic studies in fresh Mueller-Hinton broth. *Diagn Microbiol Infect Dis*, 59(3), 347–349. 10.1016/j.diagmicrobio.2007.05.013 [PubMed: 17662552]
- Scheibler E, da Silva RM, Leite CE, Campos MM, Figueiredo MA, Salum FG, & Cherubini K (2018, May). Stability and efficacy of combined nystatin and chlorhexidine against suspensions and biofilms of *Candida albicans*. *Arch Oral Biol*, 89, 70–76. 10.1016/j.archoralbio.2018.02.009 [PubMed: 29477025]
- Talapko J, Juzbasic M, Matijevic T, Pustijanac E, Bekic S, Kotris I, & Skrlec I (2021, Jan 22). *Candida albicans*-The Virulence Factors and Clinical Manifestations of Infection. *J Fungi (Basel)*, 7(2). 10.3390/jof7020079
- Willems HM, Kos K, Jabra-Rizk MA, & Krom BP (2016, Jul). *Candida albicans* in oral biofilms could prevent caries. *Pathog Dis*, 74(5). 10.1093/femspd/ftw039
- Xiao J, Hara AT, Kim D, Zero DT, Koo H, & Hwang G (2017, Jun). Biofilm three-dimensional architecture influences in situ pH distribution pattern on the human enamel surface. *Int J Oral Sci*, 9(2), 74–79. 10.1038/ijos.2017.8 [PubMed: 28452377]
- Xiao J, Huang X, Alkhers N, Alzamil H, Alzoubi S, Wu TT, Castillo DA, Campbell F, Davis J, Herzog K, Billings R, Kopycka-Kedzierawski DT, Hajishengallis E, & Koo H (2018). *Candida albicans* and Early Childhood Caries: A Systematic Review and Meta-Analysis. *Caries Res*, 52(1–2), 102–112. 10.1159/000481833 [PubMed: 29262404]

- Xiao J, Klein MI, Falsetta ML, Lu B, Delahunty CM, Yates JR 3rd, Heydorn A, & Koo H (2012). The exopolysaccharide matrix modulates the interaction between 3D architecture and virulence of a mixed-species oral biofilm. *PLoS Pathog*, 8(4), e1002623. 10.1371/journal.ppat.1002623 [PubMed: 22496649]
- Xiao J, & Koo H (2010, Jun). Structural organization and dynamics of exopolysaccharide matrix and microcolonies formation by *Streptococcus mutans* in biofilms. *J Appl Microbiol*, 108(6), 2103–2113. 10.1111/j.1365-2672.2009.04616.x [PubMed: 19941630]
- Zeng L, & Burne RA (2013, Feb). Comprehensive mutational analysis of sucrose-metabolizing pathways in *Streptococcus mutans* reveals novel roles for the sucrose phosphotransferase system permease. *J Bacteriol*, 195(4), 833–843. 10.1128/JB.02042-12 [PubMed: 23222725]
- Zeng Y, Fadaak A, Alomeir N, Wu TT, Rustchenko E, Qing S, Bao J, Gilbert C, & Xiao J (2022). *Lactobacillus plantarum* Disrupts *S. mutans*-*C. albicans* Cross-Kingdom Biofilms. *Front Cell Infect Microbiol*, 12, 872012. 10.3389/fcimb.2022.872012 [PubMed: 35392605]
- Zeng Y, Nikitkova A, Abdelsalam H, Li J, & Xiao J (2019, Feb). Activity of quercetin and kaempferol against *Streptococcus mutans* biofilm. *Arch Oral Biol*, 98, 9–16. 10.1016/j.archoralbio.2018.11.005 [PubMed: 30419487]

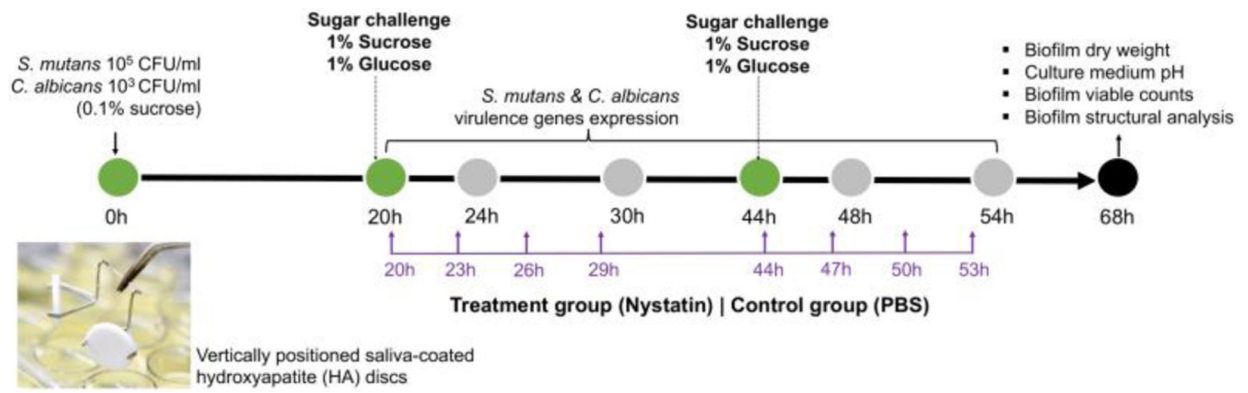


Fig. 1. Schematic study design

We used a duo species biofilm model to evaluate the effect of antifungal medications on *S. mutans* and *C. albicans* duo-species biofilm formation. Culture medium was changed once/daily at 20 and 44 hours (marked as green dot). Biofilms grew under 0.1% sucrose condition in the first 20 hours, then were subjected to sugar challenge with 1% sucrose and 1% glucose. Nystatin (treatment group) and PBS (control group) applications were administered 4 times/day, 5 minutes/application, between 20–68 hours (marker in purple).

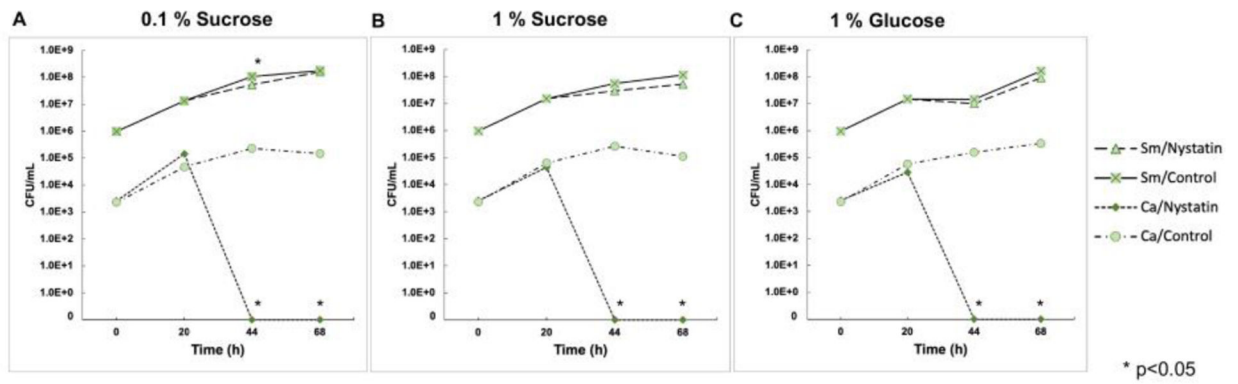


Fig. 2. Effect of Nystatin on *S. mutans* and *C. albicans* viability in duo-species biofilms. Viable cells of *S. mutans* and *C. albicans* were assessed using colony forming unit (CFU). (A) 0.1% sugar condition, (B) 1% sucrose condition, and (C) 1% glucose condition. Viable *C. albicans* were undetected after 44 hours of biofilm formation in all sugar conditions. The abundance of *S. mutans* was reduced by 0.5 log CFU/ml at 44 and 68 hours in the Nystatin-treated group with 1% sucrose, ($p=0.03$, *t-test*).

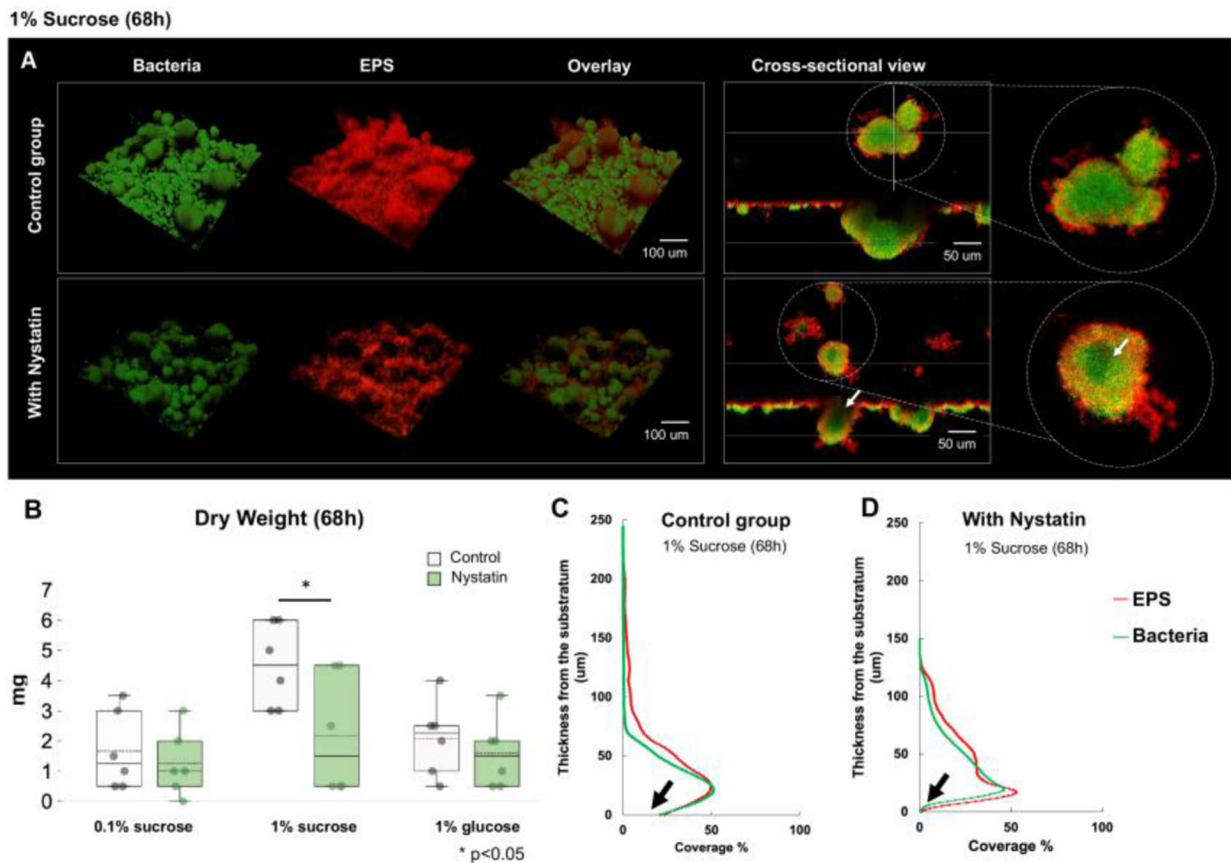


Fig. 3. Morphogenesis and 3D architecture of *S. mutans* and *C. albicans* duo-species biofilms treated by Nystatin

(A) Morphogenesis and 3D architecture of 68h Nystatin-treated biofilms were visualized. Altered biofilm structures were seen, with smaller and hollow microcolonies. White arrow indicates inner aspect of microcolony. (B) Significant reduction of biofilm dry weight following Nystatin treatment was seen in 1% sucrose condition, comparing to the control group, ($p=0.04$, *t-test*). (C-D) Layer distribution of the 68h biofilms formed in 1% sucrose showed that the Nystatin-treated biofilms had thinner layers and with less biomass at the substrate layer (marked with black arrows).

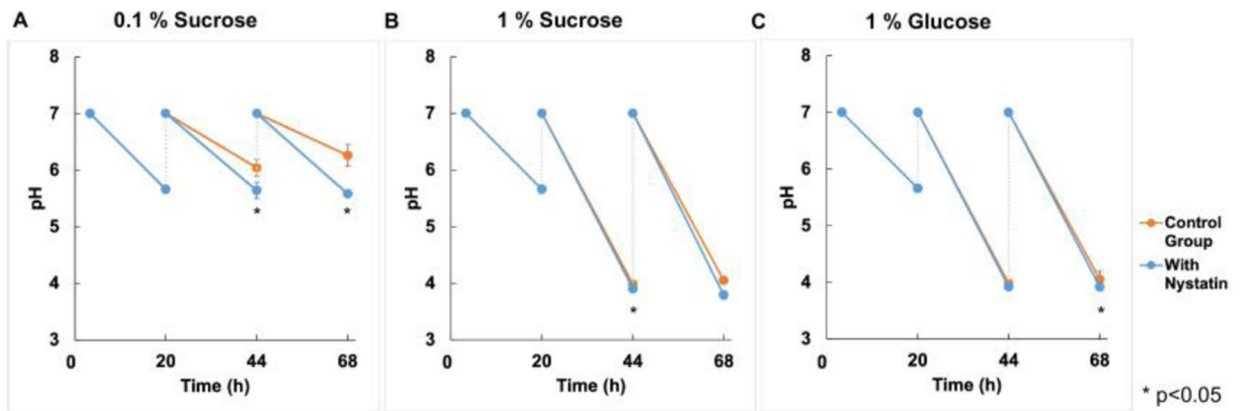
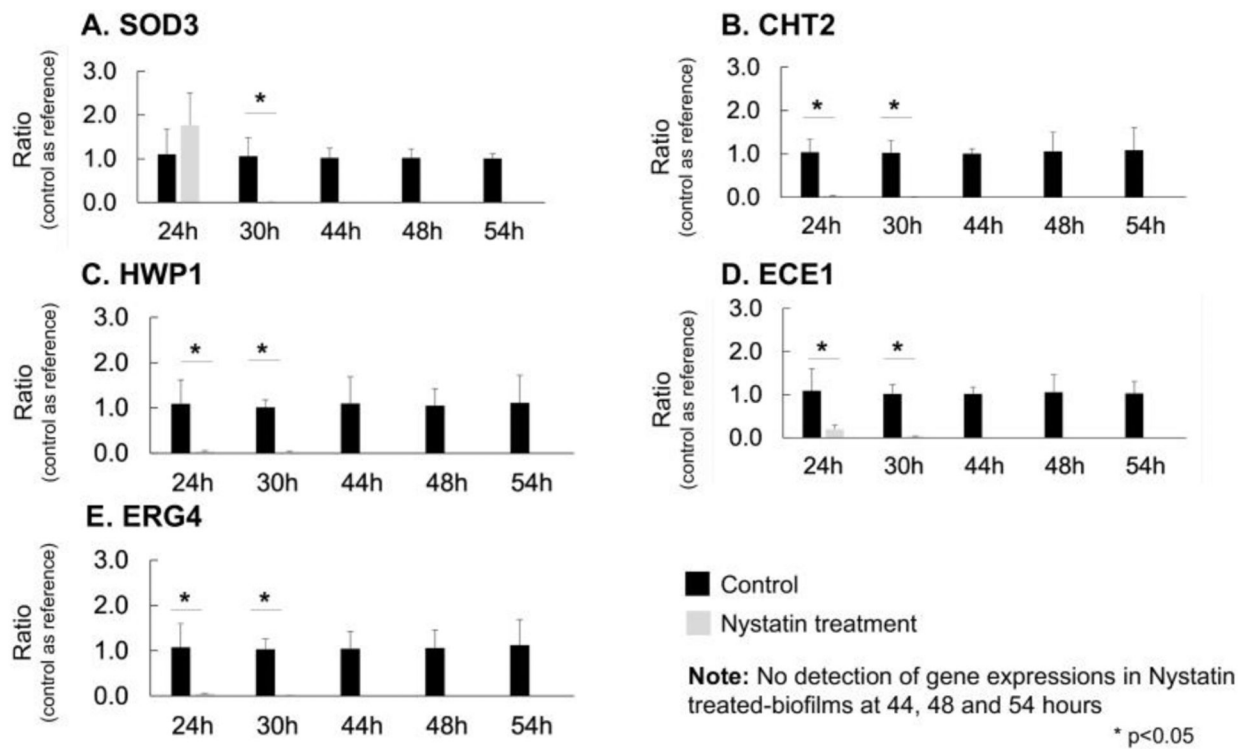
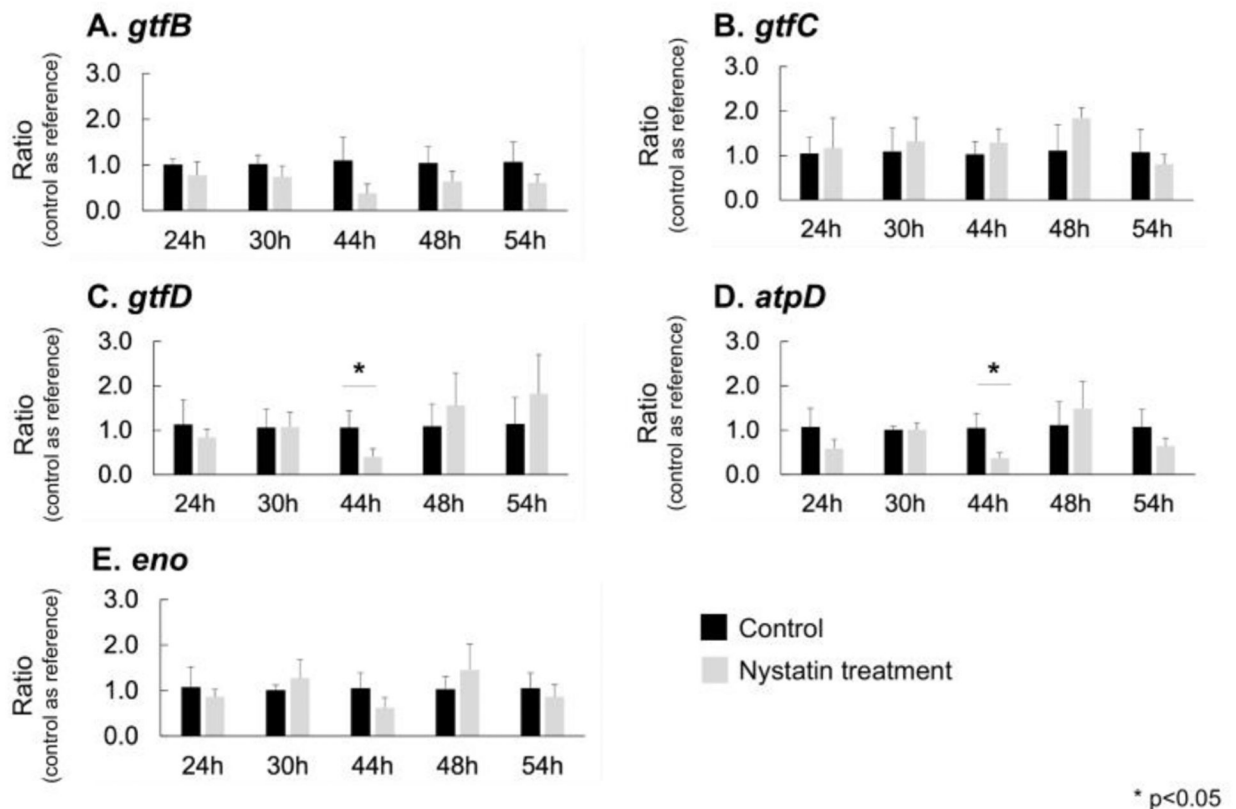


Fig. 4. pH value in culture media

(A) The pH value of culture medium was significantly lower in the Nystatin treated group comparing to the control group at 44 and 68 hours under 0.1% sucrose sugar conditions, ($p < 0.001$, *t-test*). (B-C) No significant reduction was noted in 1% sucrose and 1% glucose conditions.

***C. albicans* gene expression****Fig. 5. Expression of *C. albicans* virulence genes**

The real-time PCR was performed to assess *C. albicans* virulence genes. *CHT2*, *HWP1*, *ECE1*, and *ERG4* were significantly down-regulated ($p < 0.05$, *t*-test) immediately following the first Nystatin application at 24h. *SOD3* gene was significantly down-regulated ($p < 0.05$, *t*-test) after 30 hours. At 44 hours which is after 4 applications of Nystatin, the expressions of all *C. albicans* virulence genes were not detectable.

***S. mutans* gene expression**

* p<0.05

Fig. 6. Expression of *S. mutans* virulence genes

The real-time PCR was performed to assess *S. mutans* virulence genes. The biofilms treated with Nystatin had down-regulations of *gtfB*, and *eno* genes, compared to the control group, despite no statistically significant differences were detected. The expression of *S. mutans gtfD* and *atpD* was significantly down-regulated ($p < 0.05$, *t-test*) in the Nystatin-treated biofilms than the control group at 44 hours when 4 Nystatin applications had been administered ($p < 0.05$, *t-test*)

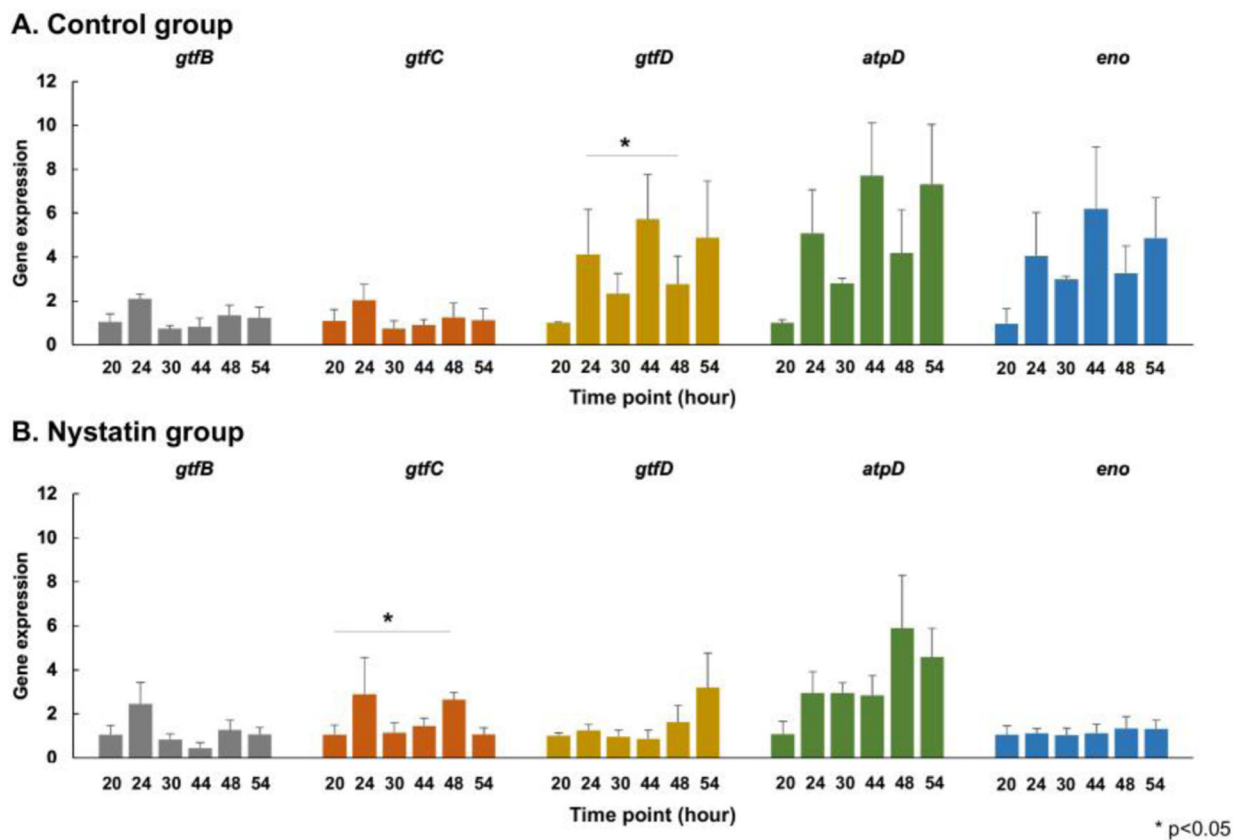


Fig. 7. Dynamic changes of *S. mutans* virulence genes in control and Nystatin-treated *S. mutans* and *C. albicans* duo-species biofilms

The dynamic expressions of *S. mutans* virulence genes in the control (A) and Nystatin-treated biofilms (B) were assessed. No significant change was seen in the dynamic expression of *gtfB*, *atpD*, and *eno* genes in both the control and Nystatin-treatment group. However, there was a significant change in the dynamic expression of *gtfD* in the control group and a significant change in the dynamic expression of *gtfC* in the Nystatin-treated biofilms. (p<0.05, repeated ANOVA).

Table 1.

Quantitative assessment of microcolonies in mixed species biofilms

Parameters	Control group	Nystatin group	P-value
Substate-attached microcolonies			
Number	7.3±3.7	1.8±1.7	0.04*
Area (µm²) ×10³	2.1±2.6	0.2±0.1	0.13
Volume (µm³) ×10⁶	1.9±1.3	3.7±1.6	0.89
Floating microcolonies			
Number	235.4±142.2	200.8±47.2	0.48
Diameter (µm)	42.9±8.7	36.2±3.2	0.04*
Volume (µm³) ×10³	6.9±7.8	8.9±9.	0.62

Values are represented as means ±SD

*
p<0.05

Author Manuscript

Author Manuscript

Author Manuscript

Author Manuscript